BJRS

BRAZILIAN JOURNAL
OF
RADIATION SCIENCES
10-01 (2022) 01-13

SBPR
Sociedade Brasileira de Proteção Radiológica

On development of in-core fuel system for PWR reactors: Part I generation of macroscopic cross sections using SCALE 6.0 for use in nodal calculation

Rodrigues[1] P.H.S, Maiorino[2] J.R., Asano JR.[3] R.

[1]PhD Student in the Graduate Program on Energy, UFABC, Santo André, Brazil, pedro.rodrigues@ufabc.edu.br; [2]Professor in the Graduate Program on Energy, UFABC, Santo André, Brazil, joserubens.maiorio@ufabc.edu.br; [3]Researcher in the Graduate Program on Energy, UFABC, Santo André, Brazil roberto.asano@ufabc.edu.br

ABSTRACT

This work presents the description of the first part of a methodology applied to perform In-Core Fuel Management (ICFM) in Pressurized Water Reactor (PWR). The ICFM of a PWR reactor consists on defining the best charging or recharging pattern of fuel assemblies inside a reactor for an operational cycle. This means, finding a suitable arrangement of fuel assemblies that optimizes the performance of the reactor, which complies with all safety criteria. Genetic algorithms (GAs) are used to select the arrangements that interact with the reactor physics simulation code, holding the neutron characteristics of each fuel assembly. Therefore, a reliable and fast code was developed accordingly. The consolidated technique of coarse mesh node code that numerically solves the multigroup diffusion equation for two groups of energy, fast and thermal neutrons, in two dimensions was selected. In this type of code, it is essential that each fuel assembly is homogenized and characterized by its macroscopic cross sections, for each reactor's burnup condition. The cross sections are generated with the support of NEWT, ORIGEN and TRITON modules in SCALE 6.0, a computational platform developed by the Reactor and Nuclear Systems Division (RNSD), from the Oak Ridge National Laboratory (ORNL). The completeness of the qualification and validation of the results obtained from the homogenization of the fuel assembly by the SCALE was performed comparing the infinity multiplication factor results with actual data of a benchmark reactor. The fully documented Almaraz Nuclear Power Plant provided by the International Atomic Energy Agency (IAEA)-TECDOC-815, has been used as benchmark with successful results.

Keywords: in-core fuel management, PWR, benchmark, SCALE.

ISSN: 2319-0612
Accepted: 2021-10-15

1. INTRODUCTION

Nuclear fuel management relates to the decisions pursuing the optimal strategy of fuel assembly (FA), replacement and reposition after each cycle of operation. It is comprising three decisions: the choice of FA that are exhausted and will be withdrawn after an operational cycle; the position or reposition of the partially burnt fuel assemblies and the type and position of new FA to be inserted in the reactor. This operation is aimed to restore reactivity for a new operational cycle, optimizing the performance of the reactor and complying with all safety criteria. This whole process is known as In-Core Fuel Management (ICFM) [1].

The ICFM is a complex optimization problem of difficult solution to Nuclear Engineering. In the early days of nuclear technology (1960's), these decisions were performed based on the experience and knowledge of the experts. In the following years, traditional optimization techniques were used, such as the gradient method [2]. With the introduction of artificial intelligence techniques, such as Genetic Algorithms (GAs), these techniques began to be applied in nuclear fuel management and they are currently becoming one of the main tools for ICFM [2].

In order to model and evaluate the ICFM, a validated reactor physics code is required. This calculation code, which shall be very efficient (low computational time usage) due to large number of variables, constrains and viable solutions, interacts with the optimization algorithm [1]. Therefore, a 2-dimensional (2D) coarse mesh nodal code was developed solving the neutron diffusion equation with two energy groups, fast and thermal neutrons.

Inside the core of an active PWR reactor, there are several types of FAs with different enrichments, concentrations, burnable poisons and burnup condition. Besides the FAs, the reactor operation is highly influenced by parameters such as fuel and moderator temperatures and boron concentration. Under these various conditions, the NEWT, ORIGEN and TRITON modules in SCALE 6.0 code was used to homogenize the FAs characteristics based on the reactor's construction parameters and its operation condition. SCALE 6.0 is able to evaluate FAs cross sections in two energy groups, which are used as parameters in the nodal code developed along this research.

To validate the generated cross sections, an IAEA benchmark was used [3]. This benchmark presents calculations and experimental data from the Nuclear Power Plant Almaraz II, currently in operation in Spain, which has a 2686MWth thermal reactor. The published benchmark does not

present the cross sections of the FAs, but describes the reactor operation, the position of the FAs at the beginning of reactor's life (BOL) and the k_∞ (infinity multiplication factor) calculations of each one of the six FAs presented in the benchmark, that will be used to compare with the calculations performed by SCALE 6.0.

The goal of this part of the research was presents a comparison between k_∞ values aiming to evaluate the used methodology to generate the homogenized macroscopic cross sections, parameters of a PWR reactor FA. These parameters will be used in the creation of a master library containing the cross sections of each type of FA at different burnup level, from new to exhaustion (after many burning steps). This library is aimed to be used in the evaluation of the nodal algorithm, coupled with an ICFM module.

This paper is organized as follows: the next section presents the Material and Methods used in this work. Results and Discussion are presented in Section 3, and the conclusions can be found on Section 4.

2. MATERIALS AND METHODS

The elaboration of the library with the FAs' cross sections for various operating conditions is a very important step for the evaluation of the nodal code used in ICFM [4]. In order to determine these cross sections it is necessary to collect operational data, dimensions and actual materials that compose each FA. Therefore, the cross sections of the FA's Almaraz II were generated using the SCALE 6.0 developed by the Reactor and Nuclear Systems Division (RNSD) from the Oak Ridge National Laboratory (ORNL) [5]. The cross sections were generated in two energy groups i.e. for fast and thermal neutrons.

The PWR core of Almaraz-II power plant has 157 fuel assemblies. The distribution of fuel assemblies in the symmetric quarter of the reactor core in the BOL is shown in Fig. 1. Each FA has 264 fuel rods arranged in the form of 17 × 17 rods' slots, some of which has 12, 16 or 20 burnable poison rods (BPR). The structure of FA with BPR is shown in the Fig. 2 and Table 1 show additional data from Almaraz-II core [3].

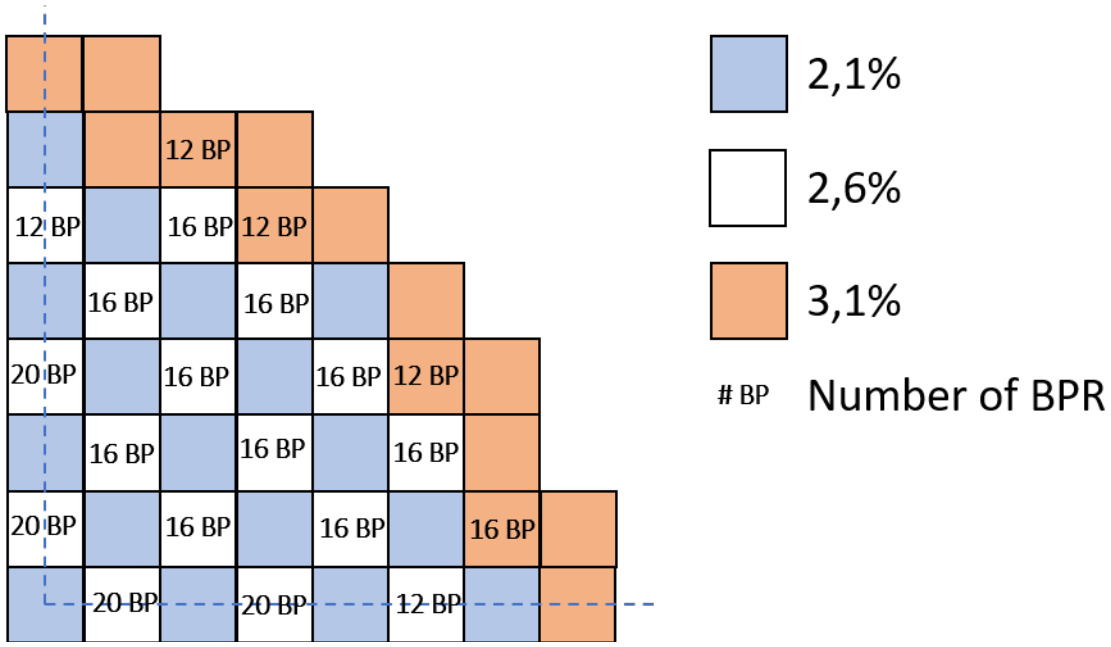

Figure 1: *The distribution of fuel assemblies in a symmetric quarter of Almaraz-II reactor's core*
Source: adapted from IAEA Almaraz-II Benchmark [3].

Table 1: Operational Conditions of Almaraz II

Thermal Power	2686 MW
Number of loops	3
Heat generated in fuel	97,4%
System nominal pressure	155 bar
Mass flow of coolant	$1{,}38.10^4$ kg/s
HFP inlet temperature	291,4 ºC
HFP average core outlet temperature	326 ºC
HFP average moderator temperature	309,9 ºC
HFP average fuel cladding temperature	340 ºC
HFP average fuel temperature	654 ºC
HFP and BOL effective fuel temperature	640 ºC
Total fuel (UO_2) loading in the core	81.856 kg

Source: IAEA Almaraz-II Benchmark [3].

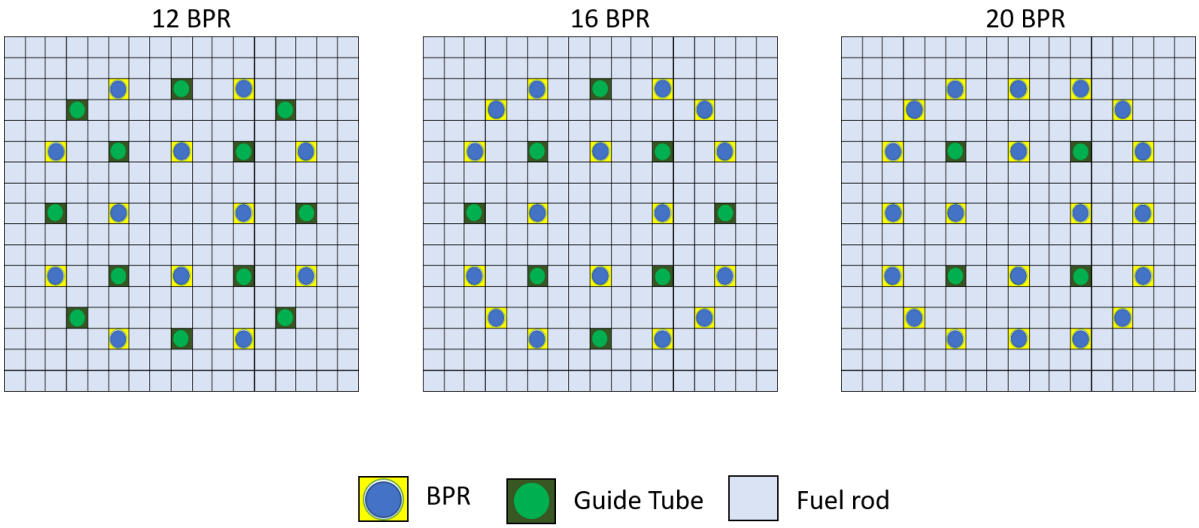

Figure 2: *Burnable poison rod position in each FA*

Source: adapted from IAEA Almaraz-II Benchmark [3].

As shown in Figure 1, the Almaraz II core has seven types of FAs with three different enrichments values, 2.1%, 2.6% and 3.1% in the first core recharge. The element with 2.6% enrichment can have a configuration with 12, 16 or 20 rods with PYREX burnable poisons while the element with 3.1% enrichment can have only 12 or 16 BPR. The position of the BPR in the elements is illustrated in Fig. 2 and the details of FA's composition and dimensions are shown in the Table 2.

There are six institutes representing the countries that participated in Almaraz II benchmark: Spain, India, South Africa, Turkey, Croatia and Serbia. Each of them evaluates the value of k_∞ in a different way for each FA. The results from this research were compared to the average (avg.) of the evaluations performed in each country, along with their respective standard deviation (std.). In order to include more recent data from the Almaraz II IAEA benchmark, the results of this work were also compared with the work of Pinem, Sembiring and Surbakti, 2019 [4], evaluated with SRAC2006 program package [6].

Previous publications, [3], only present the results of the calculations for the FAs listed in Table 3, which are the ones presented for comparison purposes. Although, FAs cross sections have been generated for all types of FAs that could be used for the calculation of the burning steps of the reactor's complete core.

In this paper, we will present the comparisons between the results of the following elements without burnup (fresh conditions) and in five other operating conditions listed in Table 4, in addition to two different levels of boron concentration, 0 ppm and 1000 ppm of boron were considered. Depletion calculations will also be presented in reactor operating condition C, which represents its condition in Hot Full Power (HFP).

Table 2: FA's composition and Dimensions

Pellet:	
Material	UO_2
Theoretical density (g/cm³)	10.97
Density (theoretical %)	95%
Radius (cm)	0.4096
Pellet length (cm)	1.346
Height UO2 (cm)	365.76
Burnable Poison Rod:	
Material	Pyrex-glass
Fraction of Boron in material B_2O_3 (w/o)	12.5
Mass of ^{10}B per unit length of rod (g/cm)	0.006234
Active length (cm)	359.562
Outside Thickness (cm)	0.48387
Clad Thickness	0.04699
Clad Material	SS-304
Inner Tube Material	SS-304
Inner Tube Outside radius (cm)	0.2305
Inner Tube Thickness (cm)	0.01651

Source: adapted from IAEA Almaraz-II Benchmark [3].

Table 3: Types of FA's

FA	Enrichment (%)	Number of BPR
1	2.1	0
2	2.6	0
3	3.1	0
4	2.6	12
5	2.6	16
6	2.6	20

Source: adapted from IAEA Almaraz-II Benchmark [3].

Table 4: Operating Conditions

Operating Condition	Avg. Fuel Temp (ºC)	Effective Fuel Temperature (ºC)	Cladding Temp. (ºC)	Moderator Temp. (ºC)
A	20	20	20	20
B	291.4	291.4	291.4	291.4
C	704	640	340	309.9
D	904	840	340	309.9
E	704	640	340	279.9

Source: adapted from IAEA Almaraz-II Benchmark [3].

Since 1980, licensed regulatory bodies and research institutions around the world have used SCALE for analysis and safety projects [5]. SCALE has several computational modules including neutron transport solvers based on deterministic techniques, similar to the NEWT case and with stochastic Monte Carlo techniques, such as the KENO module [5]. In addition, SCALE has master nuclear data libraries and processing tools for calculating continuous neutron energy or discrete multigroup calculations for decay and depletion [7]. In this study, the 238-Group ENDF/B-VII.0 nuclear data was used for the calculations with SCALE 6.0.

Figure 3 (a) shows the execution sequence, using SCALE modules, known as T-XSEC. T-XSEC is used to generate the FA cross sections without depletion. The sequence T-DEPL, presented in Figure 3 (b), includes the depletion in the calculation [7]. Both sequences use some modules from the SCALE 6.0 package. Those modules are used for the treatment and processing of the cross sections. It is obtained from the neutron flux calculated deterministically, a solution from the NEWT program transport code.

The NEWT (New ESC-based Weighting Transport code) is a deterministic, 2D code that solves the neutron transport equation in a discretized mesh. It is an extremely powerful and versatile software developed based on the Extended Step Characteristic [5]. In the T-DEPL sequence, the NEWT transport calculation is followed by the depletion calculations performed by the COUPLE and ORIGEN-S modules [7]. Those modules calculate the time-dependent radioactive isotope concentration, which are simultaneously produced or depleted by neutron transmutation, fission and radioactive decay [8] and [3, 4].

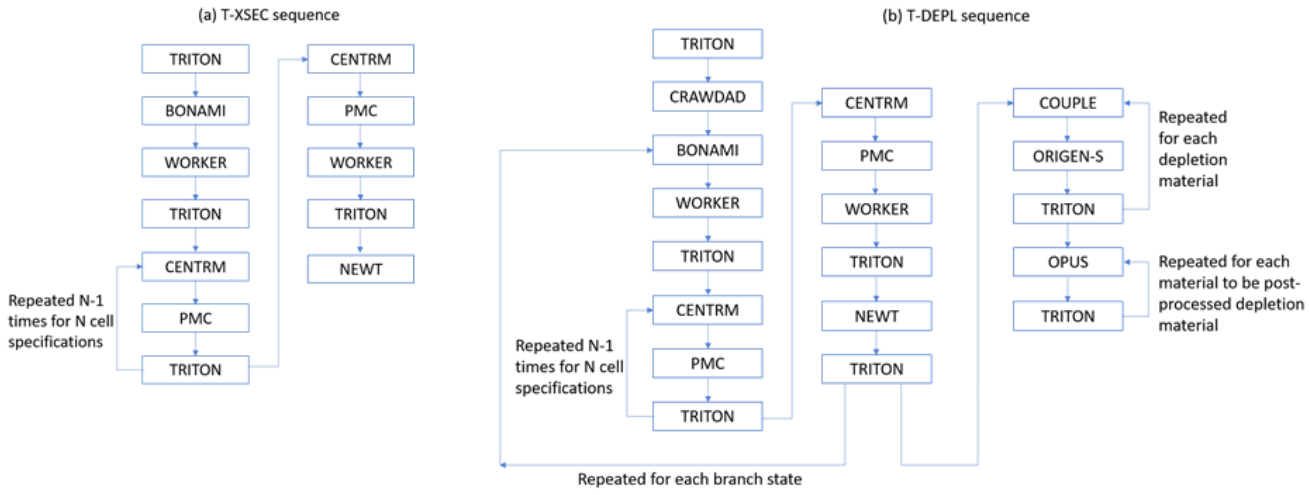

Figure 3: *(a) T-XSEC (b) T-DEPL sequence steps by SCALE 6.0 used in calculations*
Source: adapted from Rearden and Jessee, 2016 [5].

3. RESULTS AND DISCUSSION

In order to access the accuracy of the proposed method, the results were compared with the average k_∞ calculations performed by the researchers of several countries in [3], with SRAC-2006 code. The benchmark [4] not show the calculations for FAs in fresh conditions, only in depletions calculations, from the researchers from Serbia. Therefore, the average values were evaluated accordingly. All results are shown in Table 5 for FA type (% enrichment) with 0 ppm of boron for each operational condition (T), listed in Table 4. The IAEA benchmark column shows the average calculations from IAEA benchmark with their respective standard deviation (Std.). The SCALE 6.0 column shows the k_∞ calculations performed with the proposed method of this work at the following conditions: average fuel temperature (T_{avg}) and effective fuel temperature (T_{eff}). Table 5 also shows the temperature dependent difference between SCALE calculation and IAEA benchmark reactivities ($\Delta\rho_1$) as well as between SCALE and SRAC-2006 results ($\Delta\rho_2$).

Table 5: Comparation of k_∞ values for each operating condition (T) with 0 ppm of boron.

FA with 2,1% enrichment									
	IAEA benchmark		**SRAC**	**SCALE**		$\Delta\boldsymbol{\rho_1}$		$\Delta\boldsymbol{\rho_2}$	
T	k_∞(avg.)	Std. (pcm)	k_∞	$k_\infty\ (T_{avg})$	$k_\infty\ (T_{eff})$	$\Delta\rho_1(T_{avg})$ (pcm)	$\Delta\rho_1(T_{eff})$ (pcm)	$\Delta\rho_2(T_{avg})$ (pcm)	$\Delta\rho_2(T_{eff})$ (pcm)
A	1.288512	491	1.29695	1.299678	-	667	-	162	-
B	1.251546	669	1.25933	1.262686	-	705	-	211	-
C	1.232560	702	1.23875	1.242314	1.244508	637	779	232	373
D	1.226296	671	1.23285	1.236771	1.238372	691	795	257	362
E	1.242540	571	1.24856	1.251970	1.254107	606	742	218	354
FA with 3,1% enrichment									
	IAEA benchmark		**SRAC**	**SCALE**		$\Delta\boldsymbol{\rho_1}$		$\Delta\boldsymbol{\rho_2}$	
T	k_∞(avg.)	Std. (pcm)	k_∞	$k_\infty\ (T_{avg})$	$k_\infty\ (T_{eff})$	$\Delta\rho_1(T_{avg})$ (pcm)	$\Delta\rho_1(T_{eff})$ (pcm)	$\Delta\rho_2(T_{avg})$ (pcm)	$\Delta\rho_2(T_{eff})$ (pcm)
A	1.396078	552	1.40479	1.405562	-	483	-	39	-
B	1.349588	759	1.35746	1.359229	-	526	-	96	-
C	1.328142	804	1.33430	1.336727	1.338973	484	609	136	262
D	1.321486	764	1.32810	1.331123	1.332718	638	638	171	261
E	1.340750	646	1.34689	1.349148	1.351333	464	584	124	244
FA with 2,6% enrichment									
	IAEA benchmark		**SRAC**	**SCALE**		$\Delta\boldsymbol{\rho_1}$		$\Delta\boldsymbol{\rho_2}$	
T	k_∞(avg.)	Std. (pcm)	k_∞	$k_\infty\ (T_{avg})$	$k_\infty\ (T_{eff})$	$\Delta\rho_1(T_{avg})$ (pcm)	$\Delta\rho_1(T_{eff})$ (pcm)	$\Delta\rho_2(T_{avg})$ (pcm)	$\Delta\rho_2(T_{eff})$ (pcm)
A	1.350510	515	1.35908	1.360704	-	555	-	88	-
B	1.308166	705	1.31597	1.318458	-	597	-	143	-
C	1.287706	748	1.29389	1.296824	1.299051	546	678	175	307
D	1.281188	713	1.28781	1.291241	1.292834	608	703	206	302
E	1.298802	622	1.30529	1.308058	1.310225	545	671	162	289
FA with 2,6% enrichment with 12 BRP									
	IAEA benchmark		**SRAC**	**SCALE**		$\Delta\boldsymbol{\rho_1}$		$\Delta\boldsymbol{\rho_2}$	
T	k_∞(avg.)	Std. (pcm)	k_∞	$k_\infty\ (T_{avg})$	$k_\infty\ (T_{eff})$	$\Delta\rho_1(T_{avg})$ (pcm)	$\Delta\rho_1(T_{eff})$ (pcm)	$\Delta\rho_2(T_{avg})$ (pcm)	$\Delta\rho_2(T_{eff})$ (pcm)
A	1.215512	869	1.21908	1.218078	-	173	-	-67	-
B	1.149202	920	1.15420	1.154663	-	412	-	35	-
C	1.128690	867	1.13217	1.131868	1.134081	249	421	-24	149
D	1.122822	809	1.12663	1.126134	1.127804	262	393	-39	92
E	1.142472	827	1.14553	1.145051	1.147221	197	362	-37	129

Table 5: Comparation of k_∞ values for each operating condition (T) with 0 ppm of boron (continuation).

FA with 2,6% enrichment with 16 BRP									
	IAEA benchmark		**SRAC**	**SCALE**		$\Delta\rho_1$		$\Delta\rho_2$	
T	k_∞(avg.)	Std. (pcm)	k_∞	k_∞ (T_{avg})	k_∞ (T_{eff})	$\Delta\rho_1(T_{avg})$ (pcm)	$\Delta\rho_1(T_{eff})$ (pcm)	$\Delta\rho_2(T_{avg})$ (pcm)	$\Delta\rho_2(T_{eff})$ (pcm)
A	1.172882	1147	1.17870	1.177963	-	368	-	-53	-
B	1.102022	1186	1.10953	1.110426	-	687	-	73	-
C	1.081890	1128	1.08767	1.087587	1.089778	484	669	-7	178
D	1.076230	1076	1.08228	1.081881	1.083547	485	627	-34	108
E	1.095928	1111	1.10135	1.101138	1.103228	432	604	-17	155
FA with 2,6% enrichment with 20 BRP									
	IAEA benchmark		**SRAC**	**SCALE**		$\Delta\rho_1$		$\Delta\rho_2$	
T	k_∞(avg.)	Std. (pcm)	k_∞	k_∞ (T_{avg})	k_∞ (T_{eff})	$\Delta\rho_1(T_{avg})$ (pcm)	$\Delta\rho_1(T_{eff})$ (pcm)	$\Delta\rho_2(T_{avg})$ (pcm)	$\Delta\rho_2(T_{eff})$ (pcm)
A	1.131038	1328	1.13708	1.135196	-	324	-	-146	-
B	1.056936	1330	1.06483	1.064359	-	660	-	-42	-
C	1.037954	1324	1.04331	1.041588	1.043767	336	537	-158	42
D	1.031638	1206	1.03809	1.035868	1.037546	396	552	-207	-51
E	1.051224	1255	1.05708	1.055138	1.057279	353	545	-174	18

Source: author.

The results of k_∞ calculated with SCALE 6.0 at Table 5 are consistent with the expected values. In operating conditions, A, with a cooler fuel temperature, the value of k_∞ was higher than in cases B, C, D and E, which are conditions of higher temperatures. The value of k_∞ decreased as there was an increase in the number of BPR in FAs of 2.6%, once the pyrex that constitutes the BPR material has boron as a component. Boron is a neutron absorber, which reduces the FAs excess of reactivity.

Comparing the results shown in Table 5, we can conclude that the calculations presents better accuracy with average temperature T_{avg}, because the absolute value of $\Delta\rho_{1,2}(T_{avg})$ are smaller than $\Delta\rho_{1,2}$ (T_{eff}) in both comparisons, IAEA benchmark and SRAC 2006. Therefore, further calculations with T_{avg} were preferred.

It can also be noticed that the 2.1% FA has the greatest divergence between the average values of the benchmark and the values calculated by SCALE. The $\Delta\rho_1$ (T_{avg}) in case B was 705 pcm, with a percentual difference of 0.89% between the average IAEA benchmark results. In addition to that, the

value of 705 pcm was slightly beyond calculations of standard deviation between the values of the five institutes from the IAEA benchmark. With exception FA 2.1% in case A, D, E and assembly 2.6% in case A, all other calculated values were within the standard deviation values. The closest value found was in FA 2,6% with 12 BRP in case A, whose $\Delta\rho$ was 173 pcm, an error of 0.21%.

One possible cause of the difference in the values of k_∞ can be attributed to the methodology for neutron transport calculation, which is different in each nuclear code calculations and in the respective nuclear data. In this study, like the SRAC-2006 calculations, the 238-group ENDF/B-VII.0 nuclear data has been used. However, the number of neutron energy groups used in SRAC-2006 nuclear data was not reported in [4]. Despite that, if we compare the calculations of SRAC 2006 with SCALE 6.0, the results are much closer, probably due to the use of the same set of nuclear data.

Comparing the results calculated with SCALE 6.0 and SRAC-2006, it is possible to note that the greatest difference of $\Delta\rho_2\ (T_{avg})$ of 257 pcm, occurred again for 2.1% FA at operating condition D. On the other way around, considering absolute values, in FA 2.6% with 16 BRP at operational condition C, the 7 pcm $\Delta\rho_2\ (T_{avg})$ was the closest calculated value.

Thus, the results shown in Table 5 obtained by SCALE 6.0, although partially disparate from benchmark averages, were considered acceptable, based on the convergence with SRAC-2006 results.

Table 6 presents the calculated k_∞value for fuel assemblies, with same operational conditions as shown in Table 5, but, in this case, considering the addition of 1000 ppm of soluble boron.

Similar to the previous case with no boron, the values of k_∞ calculated with SCALE 6.0, shown in Table 6, are also consistent with the expected results, because soluble boron, as a neutron absorber, would decrease the reactivity of the FA. We can also conclude the calculations had a better accuracy when the average temperature T_{avg} was used.

It is remarkable that the standard deviation of the values presented in the benchmark with BRP and 1000 ppm of soluble boron is higher in relation to the average. Standard deviation is in the order of 700 pcm for the case of 12 BPR, and about 1000 pcm for the cases with 16 or 20 BPR. Thus, all results from SCALE 6.0 calculations presented in Table 6 are within the standard deviation of the benchmark, with an absolute maximum value of $\Delta\rho_1(T_{avg})$ equal to 565 pcm, in the case of FA with 2.6% enrichment and with 20 BRP (case B). The maximal difference to the SRAC-2006 calculated values is 472 pcm for the same FA, but in case D.

Table 6: Comparation of k_∞ values for each operating condition (T) with 1000 ppm of boron

FA with 2,1% enrichment – 1000 ppm									
	IAEA benchmark		**SRAC**	**SCALE**		$\Delta\boldsymbol{\rho_1}$		$\Delta\boldsymbol{\rho_2}$	
T	k_∞(avg.)	Std. (pcm)	k_∞	$k_\infty\ (T_{avg})$	$k_\infty\ (T_{eff})$	$\Delta\rho_1(T_{avg})$ (pcm)	$\Delta\rho_1(T_{eff})$ (pcm)	$\Delta\rho_2(T_{avg})$ (pcm)	$\Delta\rho_2(T_{eff})$ (pcm)
A	1.072382	490	1.07438	1.074983	-	226	-	52	-
B	1.089856	555	1.09276	1.093851	-	335	-	91	-
C	1.080572	586	1.08237	1.082374	1.084536	154	338	0	185
D	1.075022	576	1.07717	1.076744	1.078389	149	290	-37	105
E	1.078024	494	1.07920	1.078766	1.080878	64	245	-37	144
FA with 3,1% enrichment – 1000 ppm									
	IAEA benchmark		**SRAC**	**SCALE**		$\Delta\boldsymbol{\rho_1}$		$\Delta\boldsymbol{\rho_2}$	
T	k_∞(avg.)	Std. (pcm)	k_∞	$k_\infty\ (T_{avg})$	$k_\infty\ (T_{eff})$	$\Delta\rho_1(T_{avg})$ (pcm)	$\Delta\rho_1(T_{eff})$ (pcm)	$\Delta\rho_2(T_{avg})$ (pcm)	$\Delta\rho_2(T_{eff})$ (pcm)
A	1.207354	488	1.20950	1.208423	-	73	-	-74	-
B	1.212668	640	1.21581	1.215935	-	222	-	8	-
C	1.200068	677	1.20195	1.201528	1.203758	101	255	-29	125
D	1.194020	658	1.19635	1.195796	1.197459	124	241	-39	77
E	1.201144	558	1.20253	1.201632	1.203807	34	184	-62	88
FA with 2,6% enrichment – 1000 ppm									
	IAEA benchmark		**SRAC**	**SCALE**		$\Delta\boldsymbol{\rho_1}$		$\Delta\boldsymbol{\rho_2}$	
T	k_∞(avg.)	Std. (pcm)	k_∞	$k_\infty\ (T_{avg})$	$k_\infty\ (T_{eff})$	$\Delta\rho_1(T_{avg})$ (pcm)	$\Delta\rho_1(T_{eff})$ (pcm)	$\Delta\rho_2(T_{avg})$ (pcm)	$\Delta\rho_2(T_{eff})$ (pcm)
A	1.148652	487	1.15070	1.150376	-	130	-	-24	-
B	1.159612	594	1.16264	1.163184	-	265	-	40	-
C	1.147984	528	1.15031	1.150083	1.152288	159	325	-17	149
D	1.143860	874	1.14488	1.144377	1.146037	39	166	-38	88
E	1.147160	377	1.14919	1.148493	1.150645	101	264	-53	110
FA with 2,6% enrichment with 12 BRP – 1000 ppm									
	IAEA benchmark		**SRAC**	**SCALE**		$\Delta\boldsymbol{\rho_1}$		$\Delta\boldsymbol{\rho_2}$	
T	k_∞(avg.)	Std. (pcm)	k_∞	$k_\infty\ (T_{avg})$	$k_\infty\ (T_{eff})$	$\Delta\rho_1(T_{avg})$ (pcm)	$\Delta\rho_1(T_{eff})$ (pcm)	$\Delta\rho_2(T_{avg})$ (pcm)	$\Delta\rho_2(T_{eff})$ (pcm)
A	1.053918	852	1.05489	1.053108	-	-73	-	-160	-
B	1.036952	785	1.04011	1.039155	-	204	-	-88	-
C	1.024200	741	1.02611	1.023663	1.025811	-51	153	-233	-28
D	1.018866	680	1.02111	1.017996	1.019664	-84	77	-300	-139
E	1.027850	664	1.02916	1.026331	1.028010	-144	15	-268	-109

Table 6: Comparation of k_∞ values for each operating condition (T) with 1000 ppm of boron (continuation)

FA with 2,6% enrichment with 16 BRP – 1000 ppm									
	IAEA benchmark		**SRAC**	**SCALE**		$\Delta\boldsymbol{\rho_1}$		$\Delta\boldsymbol{\rho_2}$	
T	k_∞(avg.)	Std. (pcm)	k_∞	$k_\infty\ (T_{avg})$	$k_\infty\ (T_{eff})$	$\Delta\rho_1(T_{avg})$ (pcm)	$\Delta\rho_1(T_{eff})$ (pcm)	$\Delta\rho_2(T_{avg})$ (pcm)	$\Delta\rho_2(T_{eff})$ (pcm)
A	1.022826	1115	1.02647	1.024670	-	176	-	-171	-
B	1.000093	942	1.00534	1.004784	-	467	-	-55	-
C	0.986656	981	0.99102	0.988880	0.990997	228	444	-218	-2
D	0.981490	924	0.98614	0.983271	0.984926	185	355	-296	-125
E	0.991166	930	0.99504	0.992533	0.994610	139	349	-254	-43
FA with 2,6% enrichment with 20 BRP – 1000 ppm									
	IAEA benchmark		**SRAC**	**SCALE**		$\Delta\boldsymbol{\rho_1}$		$\Delta\boldsymbol{\rho_2}$	
T	k_∞(avg.)	Std. (pcm)	k_∞	$k_\infty\ (T_{avg})$	$k_\infty\ (T_{eff})$	$\Delta\rho_1(T_{avg})$ (pcm)	$\Delta\rho_1(T_{eff})$ (pcm)	$\Delta\rho_2(T_{avg})$ (pcm)	$\Delta\rho_2(T_{eff})$ (pcm)
A	0.991974	1314	0.99698	0.994248	-	231	-	-276	-
B	0.963390	1186	0.97030	0.968662	-	565	-	-174	-
C	0.950342	1110	0.95580	0.952370	0.954477	224	456	-377	-145
D	0.945348	1053	0.95104	0.946787	0.948438	161	345	-472	-288
E	0.955566	1077	0.96059	0.956782	0.958840	133	357	-414	-190

Source: author.

Figures 4 to 9 show the result obtained for the value of k_∞ as a function of the fuel burnup. Each figure presents the result for one FA considering different enrichment of 2.1%, 3.1%, and 2.6%. In the case of FAs with 2.6 enrichment, four conditions are presented: without BPR and with 12, 16 and 20 BPR. All of them with 1000 ppm of soluble boron. These calculations were performed under HFP, case C of Table 4, and the results were compared with average results found in IAEA benchmark, with the respective Std., and with SRAC-2006 results [4]. Smallest and Largest differences between the k_∞ values as a function of the fuel burnup for each FAs types are shown in the Tables 7 and 8.

Analyzing the graphics shown in Fig. 4 to 9 and Tables 7 and 8, it can be observed that the k_∞ as a function of the burnup level has similar characteristics for all methods for all FA types. Some discrepancies are only noted for high burnup values, mainly for FAs with BPR, but these only occur outside the FA criticality region. In this research project, k_∞ values are not required in regions of

subcriticality. Therefore, results found as function of the burnup condition were considered acceptable.

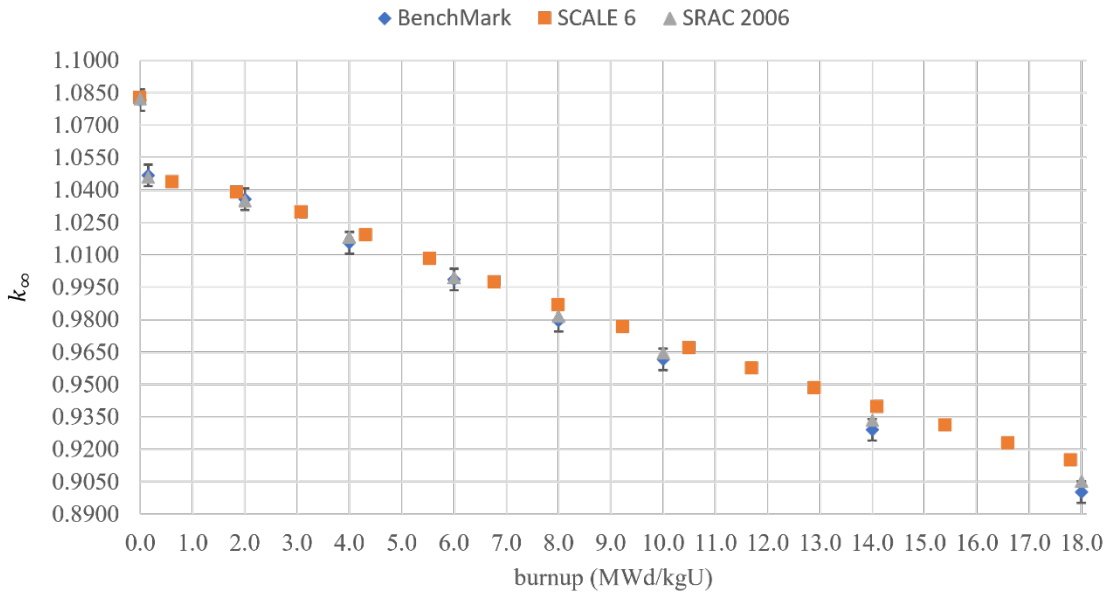

Figure 4: *k_∞ value as a function of the fuel burnup for 2.1% enrichment FA, with 1000 ppm of boron*
Source : author.

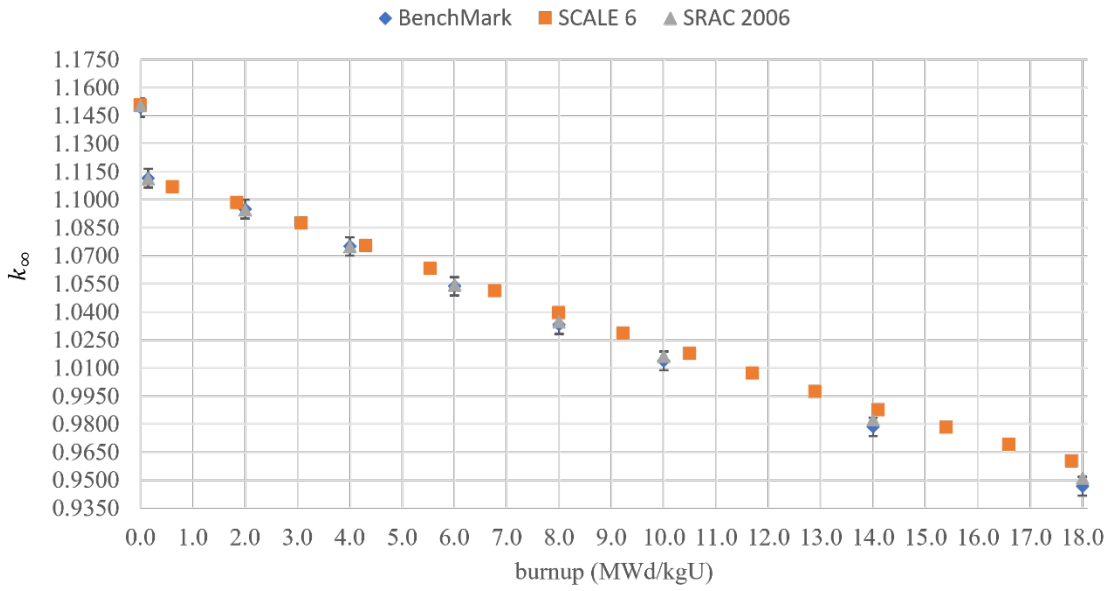

Figure 5: *k_∞ value as a function of the fuel burnup for 2.6% enrichment FA, with 1000 ppm of boron*

Source : author.

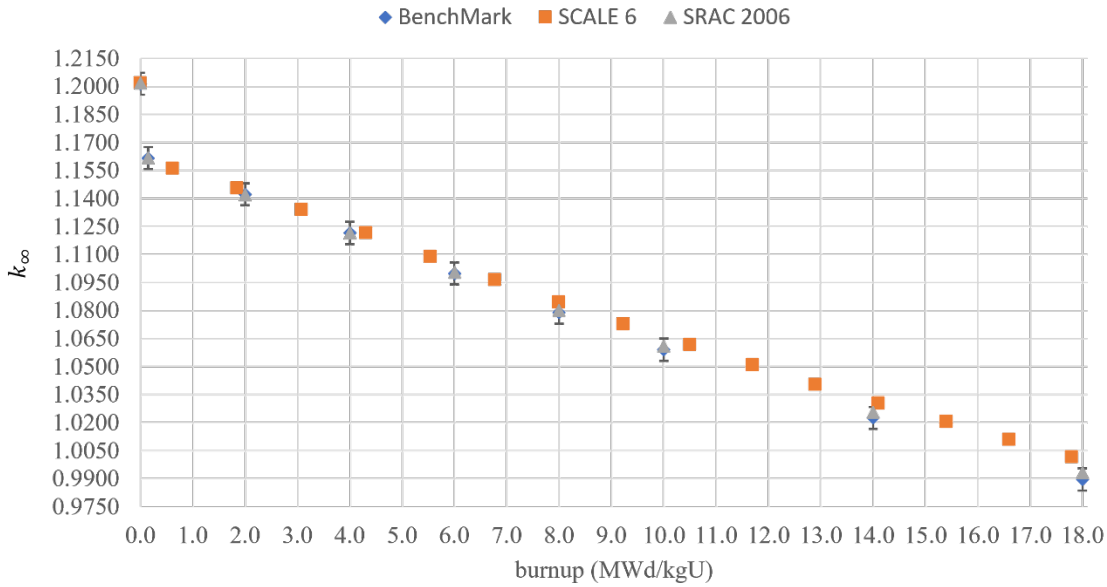

Figure 6: *k_∞ value as a function of the fuel burnup for 3.1% enrichment FA, with 1000 ppm of boron*

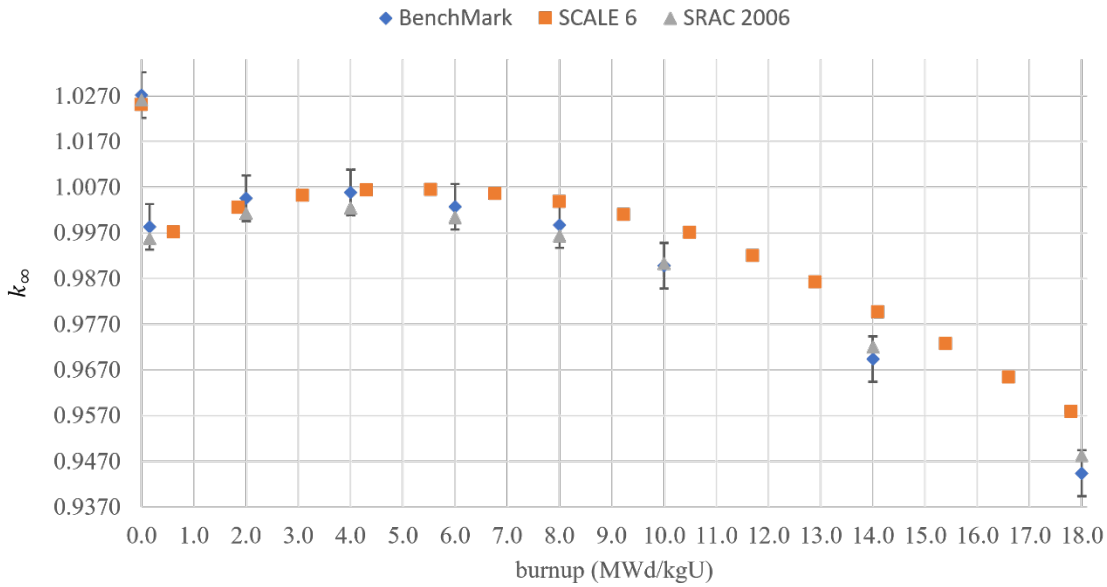

Figure 7: *k_∞ value as a function of the fuel burnup for 2.6% enrichment FA, with 12 BPR and 1000 ppm of boron*

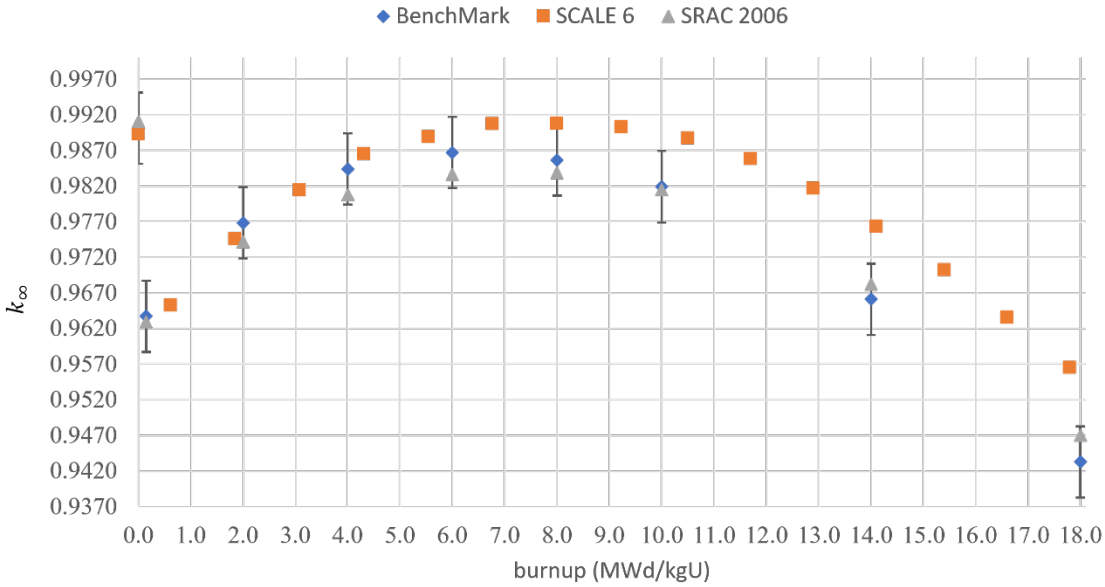

Figure 8: *k_∞ value as a function of the fuel burnup for 2.6% enrichment FA, with 16 BPR and 1000 ppm of boron*

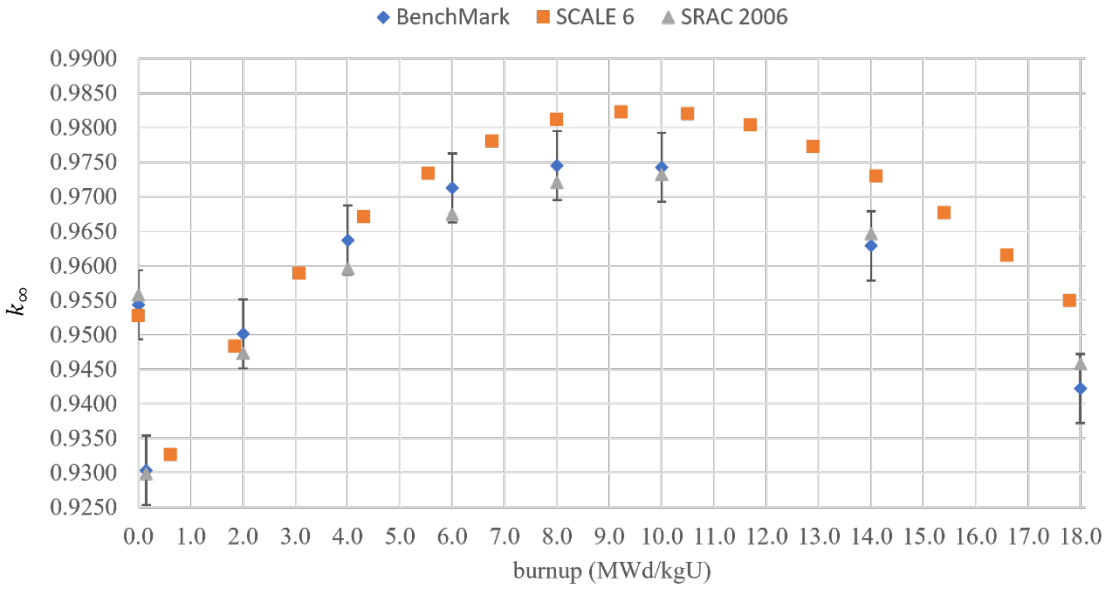

Figure 9: *k_∞ value as a function of the fuel burnup for 2.6% enrichment FA, with 20 BPR and 1000 ppm of boron*

Table 7: Smallest differences between the k_∞ values as a function of the fuel burnup for each FAs types

FAs type	**Benchmark** k_∞ (avg.)	**SRAC** k_∞	**SCALE 6** k_∞	$\Delta\rho_1$(pcm)	$\Delta\rho_2$ (pcm)
1	1.081677	1.082370	1.082762	93	33
2	1.149347	1.150320	1.150548	91	17
3	1.201487	1.201950	1.201962	33	1
4	1.027195	1.026120	1.024995	-209	-107
5	0.990087	0.991030	0.989239	-87	-183
6	0.954330	0.955800	0.952726	-176	-338

Table 8: Largest differences between the k_∞ values as a function of the fuel burnup for each FAs types

FAs type	**Benchmark** k_∞ (avg.)	**SRAC** k_∞	**SCALE 6** k_∞	$\Delta\rho_1$(pcm)	$\Delta\rho_2$ (pcm)
1	0.900200	0.905160	0.913725	1645	1036
2	0.946775	0.951090	0.958864	1332	852
3	0.989640	0.993190	1.000262	1074	712
4	0.944398	0.948280	0.956682	1360	926
5	0.943281	0.947000	0.955424	1347	931
6	0.942235	0.945790	0.953889	1297	898

It is also possible to observe in the Tables 7 and 8 that the biggest differences between the values calculated by SCALE and the benchmark values are in the calculations of FAs that have BPRs. The potential causes of the biggest differences found in these calculations, may be due to the type of modeling of the Pyrex, the material present in the BPRs, also to the differences between the way in which the modeling of these FAs in 2-D were carried out, since BPRs do not have an axially uniform distribution.

Furthermore, it is observed an expressive difference between SCALE 6.0 and SRAC-2006 depletion calculations, which was not observed in the FAs fresh conditions calculations (Table 5 and 6) results. It is difficult to know why, since both calculations use ENDF/B-VII.0. Nonetheless, probably some particular process of the depletion modules of these codes differ in the burnup calculations, but the differences in modeling or calculation methods between SCALE 6.0 and SRAC-2006 are notable in these cases and could possibly be investigated in a future work.

4. CONCLUSION

The cross sections constants for each type of FA according to its burnup level were made available with the presented methodology. As a result, the master library contained the generated macroscopic cross sections using SCALE 6.0 has been concluded with success. Considering the results obtained, the maximum difference of k_∞ value is 0.89%, between the average IAEA benchmark results and SCALE 6.0 and 0.27% between SCALE 6.0 and SRAC-2006. With such small differences, it can be concluded that the presented calculation methodology is acceptable with good accuracy, especially in the burnup conditions where FA is in critical state. Thus, SCALE 6.0 code can be used in the proposed methodology to generate the cross sections that is useful for the nodal code validation, which will be described in Part II of this work.

ACKNOWLEDGMENT

The authors thank the financial support of CAPES and UFABC and the infrastructure of the Graduate Program on Energy at UFABC.

REFERENCES

[1] P. J. Turinsky and G. T. Parks. Advances in Nuclear Fuel Management for Light Water Reactors. **Advances in Nuclear Science and Technology**, Kluwer Academic Publishers, 2002, pp. 137–165. doi: 10.1007/0-306-47088-8_6.

[2] M.L. Jayalal, S.A.V. Satya Murty, and M Sai Baba. A Survey of Genetic Algorithm Applications in Nuclear Fuel Management. **Journal of Nuclear Engineering & Technology**, vol. 4, no. 1, pp. 45–62, 2014.

[3] IAEA – International Atomic Energy Agency. **In-Core Fuel Management Code Package Validation for PWRs / IAEA-TECDOC-815**. Aug. 1995.

[4] S. Pinem, T. M. Sembiring, and T. Surbakti. Pwr Fuel Macroscopic Cross Section Analysis for Calculation Core Fuel Management Benchmark. **Journal of Physics: Conference Series**, vol. 1198, no. 2, p. 22065, Apr. 2019, doi: 10.1088/1742-6596/1198/2/022065.

[5] B. T. Rearden and M. A. S. Jessee. **SCALE Code System - ORNL/TM-2005/39**. 2016.

[6] K. Okumura, T. Kugo, K. Kaneko, and K. Tsuchihashi. **SRAC2006: A comprehensive neutronics calculation code system**. Feb. 2007.

[7] M. D. DeHart. **TRITON: A Two-Dimensional Transport and Depletion Module for Characterization of Spent Nuclear Fuel**. Jan. 2009.

[8] I. C. Gauld, O. W. Hermann, and R. M. Westfall. **ORIGEN-S: SCALE System Module to Calculate Fuel Depletion, Actinide Transmutation, Fission Product Buildup and Decay, and Associated Radiation Source Terms**. Jan. 2009.